SYSTEM SAFETY ASSESSMENT AND CONDITION MONITORING FOR AN ELECTRIC POWER TRAIN IN A TAIL ROTOR

S. Hibler*, M. Stoll†, F. Thielecke*

* Hamburg University of Technology, Institute of Aircraft Systems Engineering, Nesspriel 5, Hamburg, Germany
† Airbus Helicopters Technik GmbH, Rotor Components (ESZER) Research & Development (ESZE), Flugplatzstrasse, Calden, Germany

Abstract

The pursuit of emission-free mobility is driving the development of new propulsion concepts for rotorcraft. Electric propulsion systems are being introduced as replacements for state-of-the-art combustion engines. The usability and viability of these systems in terms of emissions, energy consumption, flight characteristics, safety and reliability, as well as costs, must be demonstrated thoroughly. A Special Condition (SC E-19) has been issued by the European Union Aviation Safety Agency (EASA) to certify electric propulsion systems. Together with the CS-27, this framework defines the conditions for the system. In this paper the special characteristics of an electric tail rotor drive are emphasized, and a safety analysis is conducted to assess the preliminary system architecture of the power train. This analysis identifies common failure modes and resulting component requirements, taking into consideration the zonal arrangement and specific risks associated with each component. The resulting requirements are used to revise the system architecture and develop a basic redundancy architecture for the electric power train. For this, preliminary failure rates are determined using Reliability Block Diagrams (RBD). Several redundancy architecture options are considered and the most promising one is selected. Critical failure modes and their probabilities of occurrence are determined using Failure Modes Effects and Criticality Analysis (FMECA), and further calculated via Fault Tree Analysis (FTA) for the resulting system architecture. Additionally, the requirements for condition monitoring within the system, including the physical signals and the associated sensors are identified.

Keywords

System Safety Assessment; Electric Power Train; Rotorcraft; HUMS

1. INTRODUCTION

The pursuit of emission-free mobility is driving the development of new propulsion concepts, which are also being considered for rotorcraft as a replacement for conventional internal combustion engines. Airbus Helicopters Technik GmbH in cooperation with Kopter Germany GmbH, MACCON GmbH & Co. KG, the German Aerospace Center (DLR) and the Institute of Aircraft Systems Engineering at the Hamburg University of Technology are investigating these new systems in the context of the "eTail" project for the tail rotor. This study focuses on exploring the necessary regulations for certification and system safety assessment associated with electric propulsion systems, along with the required Health and Usage Monitoring Systems (HUMS). The AW09 helicopter serves as the reference platform, for the development of an electric propulsion system.

2. SYSTEM DESCRIPTION

The electrification of the two main helicopter functions main rotor anti torque and yaw control is a major step towards hybrid and further on full electric flight. Analysis of the design space and simulation of flight dynamics showed possible benefits regarding power consumption, flight performance and emissions of the helicopter [1]. Demonstration of the predicted benefits for hover will be conducted by iron bird tests based on the tail boom of the Leonardo AW09. Therefore, prototypes for three concepts are developed and produced. For all concepts, the tail rotor drive (TRD) is powered by an electric motor and an electro-mechanical actuator (EMA) controls the pitch. In addition to this benchmark concept, the second concept adds an electrically articulated rudder and an enlarged fin to the configuration. With this modification it will be possible to fully stop the tail rotor in fast forward flight condition and still maintain yaw control. For the third concept, additionally vanes are added to the suction side of the tail rotor to further reduce drag in fast forward flight. Therefore, another electric actuator in forward flight conditions closes the vanes. Possible failures and subsequent failure effects of all described functions are analysed and the corresponding level of reliability is defined. The resulting degree of redundancy of each component was chosen (see section 3). Following an overview of the main functions and the involved hardware is given. Power supply is not part of the investigated system. The tail rotor is driven by an electric motor which is located at the end of the tailboom. The

doi: 10.25967/610110

power is transmitted via a conventional tail rotor shaft and the tail rotor gearbox (TGB). Since the tail rotor speed ω_{TR} is no longer coupled to the main rotor speed, it can be adjusted according to the flight condition (FC) and pilot input to minimize power consumption or noise emission. The functional flow is shown in Fig 1.

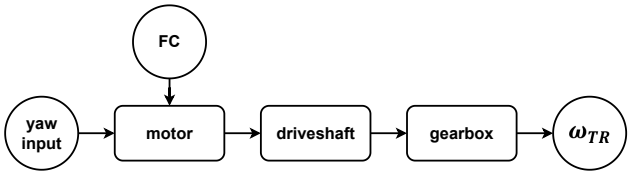

FIG 1. Functional flow of the tail rotor drive

The pitch actuation is based on the same principle, that is used in the AW09. All tail rotor blades are articulated via a rod assembly. Linkages connect this assembly to a push pull cable, which is connected to the electric actuator. Both are located inside the tail boom and the actuator is moved as far forward as possible to minimize the effect on the center of gravity. To match the rotational movement of the actuator with the required travel of the push pull cable another rod assembly is used. The functional flow from the pilots yaw input to the resulting tail rotor blade pitch θ_{TR} is shown in Fig 2.

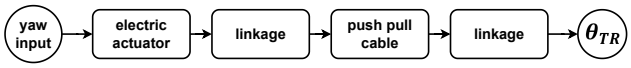

FIG 2. Functional flow of the pitch actuation

Rudder actuation of the second concept is based on the actuator design that is used for pitch adjustment. Due to lower safety requirements, a half-sized actuator is used to adjust the rudder. Via a coupling which mitigates misalignment and peak torques, the rudder is directly connected to the actuator output. The functional flow from pilot input to the changed lift coefficient C_L of the vertical fin is shown in Fig 3.

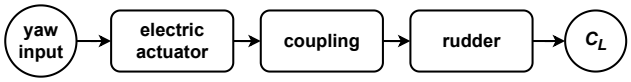

FIG 3. Functional flow for rudder movement

To cover the tail rotor vanes a similar level of safety is required as for pitch actuation. The same actuator and leverage design is used to actuate another push pull cable. The cable is connected to a second rod assembly inside the tail rotor housing. The movement of the push pull cable is transferred to a push rod, which is connected to the vanes which can cover the suction side of the rotor. To minimize the risk of false actuation, the vanes are locked in the open position by a second actuator. Only if this locking actuator opens, a movement from the vanes into their closed position is possible. Vice versa, to open the vanes, no additional action by the locking actuator is needed. It is designed so that it cannot jam the mechanism. To cover the tail rotor in flight the pilot has to actively decide to do so and be in a suitable flight condition. The functional flow is shown in Fig 4.

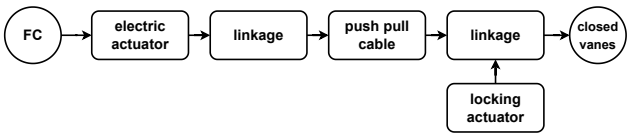

FIG 4. Functional flow to cover the tail rotor

3. SYSTEM SAFETY ASSESSMENT

To conduct the safety analysis, the SAE ARP 4761 [2] serves as the standard template for the safety assessment of civil aircraft systems and equipment. Therefore, it is utilized to identify the necessary safety and reliability requirements to meet the EASA requriements. The safety analysis results in the determination of the redundancy architecture, the predicted failure rate for the system, as well as critical failure modes.
The required failure rate for an electric helicopter system as the AW09, as per CS-27 [3], is specified as $\leq 10^{-8}\frac{1}{fh}$ for Catastrophic (CAT) events. Consequently, the Functional Development Assurance Level (FDAL) is reduced from A to B. The classifications for Hazardous (HAZ), Major (MAJ) and Minor (MIN) events remain unchanged (Tab. 1).

Criticality	Min	Maj	Haz	Cat
Failure Rate $[\frac{1}{fh}]$	10^{-3}	10^{-5}	10^{-7}	10^{-8}
FDAL	D	C	C	B

TAB 1. Criticality for Events

Another relevant document is the SC E-19 [4] which is specific to electric and hybrid propulsion systems (EHPS) in aircraft. The resulting process for designing an EHPS is given in Fig 5. Moreover, it will also be possible to certify the EHPS as a stand-alone product. The illustrated process will be carried out in its entirety in order to design the electric propulsion system in the given context.
With these regulations as the basis for certification, the safety assessment can be performed in accordance with SAE ARP 4761. The input for the assessment is the aircraft functional hazard assessment (AFHA), which determines the criticality for the corresponding flight phase. The hover and manoeuvre phases are identified as the phases in which a CAT event may occur in the event of a failure of the electric propulsion system in the tail rotor. Two main functions for the system are identified, firstly generating rotor speed and secondly changing of the pitch angle of the rotor blades.
Therefore, mitigation measures are defined for these functions. These include redundancy and possible actions, such as changing the rotor speed, that can be taken to reduce the criticality. The mitigation measures will be explained in the Failure Mode Effects and Criticality Analysis (FMECA).

3.1. Common Cause Analysis

The Common Cause Analysis (CCA) is performed in accordance with SAE ARP 4754a [6] and SAE ARP 4761. Required inputs are the architecture and the AFHA which

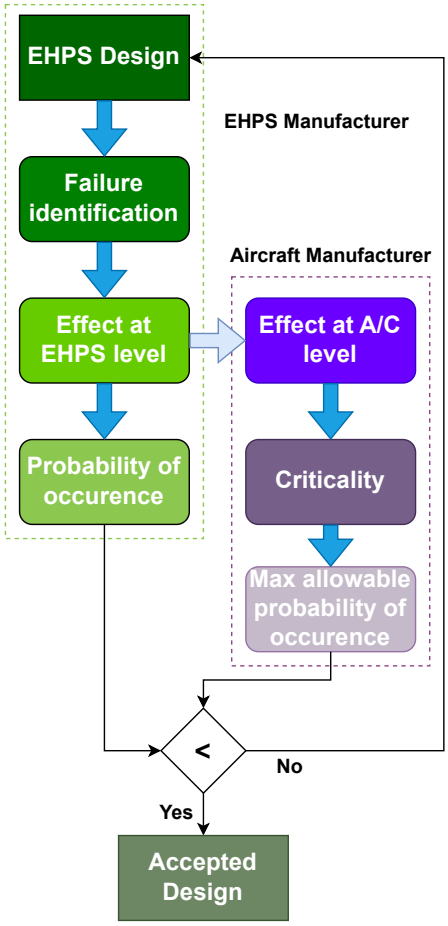

FIG 5. Process of designing an EHPS [5]

will be used in the Zonal Safety Analysis (ZSA), the Particular Risk Analysis (PRA) and the Common Mode Analysis (CMA).

3.1.1. Zonal Safety Analysis

The ZSA identifies the interactions between systems in the same installation space. The results can be used to make necessary adjustments to the system topology or the components. Zones of the reviewed system and the components are shown in Fig 6. Hazards emanating from the zones to the systems are vibrations, blocking parts, cutting edges, hot spots, significant weights, sharp edges and additional stresses. For the components the list of emanating hazards are heat, electromagnetic radiation, electrical energy, high speed rotation and vibration. With these findings and the new components described in section 2 to be integrated, a cross-check can be made for every possible permutation. The impact of vibration, significant weight and stress on the new components can be minimised with an additional safety, tensile strength calculation and appropriate shock certification for shocks in accordance with DO-160 [7]. Addressing the potential risks associated with hot spots is more complex and may require simulations to identify any necessary component repositioning or cooling strategies. The effects of electromagnetic radiation are deemed to be negligible, as the existing components in the tail rotor, such as the GPS,

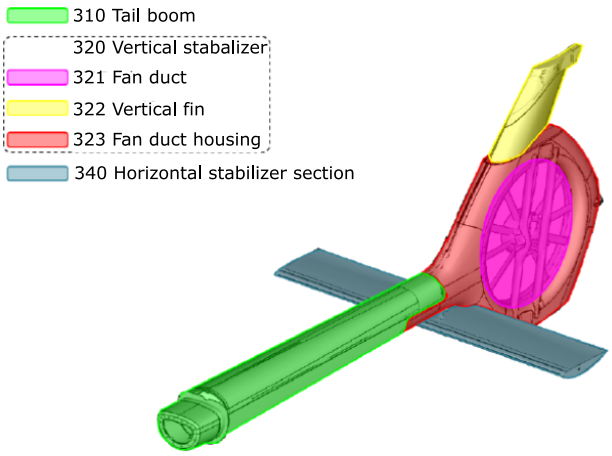

FIG 6. Zones of the tail boom

operate at a much higher frequencies compared to the newly added components and should not be affected.

3.1.2. Particular Risk Analysis

For the PRA, a list of effects that can result in an CAT event and thus need to be investigated is given in Tab. 2.

Particular Risk	Possible scenario	main feature
Bird strike	mechanical damage through kinetic energy	size, relative velocity
Fire	flammable objects and material	temperature
Parts with high kinetic energy	mechanical damage through uncontrolled rotor damage	kinetic energy through rotating components
Strong electromagnetic radiation	possible short circuit	flammability
Lightning strike	damage through electrical energy	power intensity

TAB 2. Possible particular risks

These risks must be evaluated for each installation location. The probability of an occurrence of one of these is considered low, but due to their criticality being CAT, appropriate safety measures should be set in place. Some risks may already have existing safety measures or may not be necessary to address. For example, bird strike does not have specific requirements in CS-27 due to its low probability. However, the disintegration of components with high kinetic energy is a CAT event and must be considered during component design. Electromagnetic radiation should be addressed in accordance with DO-160 standards during development and testing. For the other particular risks safety measures are already existing in the CS-27 and SC E-19 and no new ones have to be added.

It should be noted that external risks like bird or lightning strike cannot be completely excluded, but reduced with certain measures, e.g. flight planning.

3.1.3. Common Mode Analysis

The CMA is used to gain insight into redundant systems and the requirements for the Item Development Assurance Level (IDAL). This requires a redundancy architecture of the system, which is described in section 3.2 and can be represented with Reliability Block Diagrams. For the CMA in the preliminary system safety assessment (PSSA), a duplex architecture for the TRD system is considered.
Each component is transferred to the RBD and placed in its functional position. Each redundant component which is included in parallel redundant paths of the RBD is checked for common mode failures. These include software and hardware failures, environmental failures, cascading failures and common external failures. Possible options to avoid or reduce the impact of these failures are dissimilarity and barriers, component testing and maintenance, quality control and crew training. Even in the absence of common mode failures, it is possible for the system to fail if two different components fail in the different lanes. So for the redundant components the IDAL B [8] [9] is required for both components or A for one and C for the other.

3.2. Redundancy Architecture

To determine the redundancy architecture, the results of the CCA and AFHA must be taken into account, along with the component failure rates. These failure rates are sourced from the NPRD-2016 [10]. The values are generally in the same magnitude as those reported in scientific research papers, but are based on a bigger database and are therefore chosen for the calculation of the RBDs. For the RBD calculations, a constant failure rate and hot redundancy are considered. Furthermore, the possibility of applying the safe-life design on mechanical components, such as a rotor shaft, is assumed.
The failure rate F_s for two components a and b which are connected in series can be calculated according to eq.(1). The failure rate F_p for two components c and d which are connected in parallel can be calculated according to eq.(2).

$$F_s(t) = F_a(t) + F_b(t) - F_a(t) \cdot F_b(t) \tag{1}$$

$$F_p(t) = F_c(t) \cdot F_d(t) \tag{2}$$

The applied failure rates for the following calculations are given in Tab. 3.

3.2.1. Benchmark System Redundancies

To define the necessary redundancy, it is useful to obtain the failure rate of the base system without any redundant components. A failure rate of $2.13 \cdot 10^{-4} \frac{1}{fh}$ is achieved for the whole system. Examining the tail rotor drive and pitch control subsystems, the failure rates are $7.3 \cdot 10^{-5} \frac{1}{fh}$ and $1.4 \cdot 10^{-4} \frac{1}{fh}$, respectively. Analyzing the failure rates of the individual components, it is evident that no component can meet the demanded failure rate of CAT, except those designed for a safe-life. With these findings, a basic duplex redundancy is at least required for the systems.
An EMA with an internal double redundancy is used for the pitch adjustment [1]. The failure rate for this actuator is given as $10^{-12} \frac{1}{fh}$ without consideration of power electronics. Assuming a duplex architecture for the power electronics, resulting in individual lanes for each half of the actuator the failure rate calculates to $9.16 \cdot 10^{-9} \frac{1}{fh}$.

Event	Applied failure rate $[10^{-6} \frac{1}{fh}]$
Encoder Failure	6.24
Actuator Control Unit Failure	55.5
ACU Software Failure	23.87
Power Drive Electronics Failure	12.43
Power Supply Unit Failure	20.5
Sort Circuit Unit Failure	0.29
Ball Bearing Failure	1.37
Ball Joint Failure	1.05
Sleeve Bearing Failure	6.22
Winding Failure	3.42
Electric Motor Failure	5.63
Motor Control Unit Failure	5.6
Gearbox Failure	4.93
EMA Failure	$1.0 \cdot 10^{-6}$
Flexball Cable Failure	$1.0 \cdot 10^{-6}$
Link Mechanism Failure	$1.0 \cdot 10^{-6}$
Structural Failure	$1.0 \cdot 10^{-6}$

TAB 3. Applied event failure rates

After conducting a sensitivity analysis on the components, the actuator control unit (ACU) has the biggest impact on the failure rate. Thus, according to eq.(2) the failure rate can be minimized by employing a parallel system architecture for the ACU. Consequently, the same decision has to be made for the inverter. If the inverter is in serial arrangement after the ACU the failure rate is $4.7 \cdot 10^{-9} \frac{1}{fh}$, if it is in a parallel arrangement it is $3.89 \cdot 10^{-9} \frac{1}{fh}$. The parallel arrangement of the inverter does not change the magnitude of the failure rate, and because of the increasing complexity of using parallel inverters, the serial arrangement is chosen. The final RBD for the pitch control is given in Fig 7.
For the calculation of the failure rate at the system level, the mechanical connection from the EMA to the rotor was assumed to be a structural componenten and therefore has the failure rate of $10^{-12} \frac{1}{fh}$. For

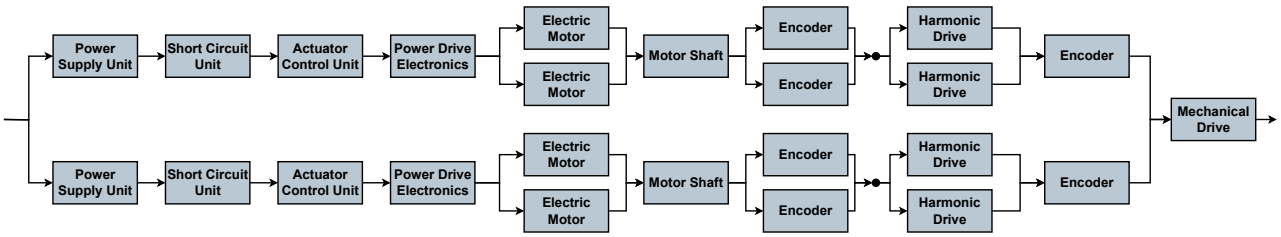

FIG 7. RBD of the pitch control system

the push pull cable, here a flexball cable, there are no published failure rates available. As it is already in use in the helicopter and not a new component. Therefore it has been thoroughly tested and is assumed to be a suitable component with a corresponding failure rate. If redundancy is still required, it can be provided by a second flexball cable connected to the same EMA.

As a first iteration step a duplex architecture is assumed for the tail rotor drive system, and calculating the failure rate for a strict duplex system yields $3.67 \cdot 10^{-9} \frac{1}{fh}$, thus meeting the threshold value for CAT events. Upon closer inspection, certain adjustments should be considered.
In a duplex configuration, the sensors used for detecting the motor's RPM may not necessarily exhibit improved performance. For instance, if one sensor starts to drift, it becomes difficult to determine which sensor is faulty. It is possible to identify the faulty sensor using analytical redundancy, where the analytical relationships of different physical parameters are known and can be used to deduce each other [11]. Alternatively, a third sensor can be incorporated, enabling the detection of the faulty sensor by the two healthy sensors. This approach effectively removes the faulty sensor from consideration (see Fig 8).

In [1] it is explained why a dual architecture of the electric motor is not feasible and a triplex architecture should be considered for the motor design in the TRD. With a triplex motor design there are several options for the lanes of the power electronics. An asymmetric design of these could be utilized, where one lane of power electronics is used to provide for two motors. This would lead to an asymmetric component sizing.
Another option is the use of three separate lanes for the power electronics. An advantage of the triplex lane is the significantly increased reliability of the power electronics system. The failure rate for the triplex TRD system is $2.63 \cdot 10^{-14} \frac{1}{fh}$, and thus below the required failure rate. But because at least two functioning lanes are necessary, the failure rate for the triplex system reduces to $3.67 \cdot 10^{-9} \frac{1}{fh}$. After consideration, the asymmetric distribution is rejected and a triplex variant is also chosen for the lanes of the power electronics.
The failure rate for the benchmark system is $1.15 \cdot 10^{-8} \frac{1}{fh}$ if the ACU is not component-wise redundant, and $7.85 \cdot 10^{-9} \frac{1}{fh}$ if it is.

As the motor in the TRD system is in a single housing, the failure rate from the NPRD-2016 may not be directly applicable for this specific component. Therefore, a closer examination of the motor is necessary. The loss of function of the motor can be divided into failure of the power electronics and sensors in the motor, the rotor, stator and bearing failure.
The failure of the power electronics doesn't change for this particular triplex motor. However, for the electric motor itself, the stator and rotor failures should be investigated. The stator failure can be categorized into structural failure and winding failure. A safe-life design approach can be assumed for the structural failure, resulting in an estimated failure rate of $10^{-12} \frac{1}{fh}$. The winding failure can be estimated through thorough testing, by application of the MIL-HDBK-217 [12], which results in a failure rate of about $10.3 \cdot 10^{-6} \frac{1}{fh}$. Another possibility is the use of failure mode distribution which states a winding failure with 31% [13] of total failures in motors and results in a failure rate of $1.75 \cdot 10^{-6} \frac{1}{fh}$. In [14] the winding failure is estimated to be $3.42 \cdot 10^{-6} \frac{1}{fh}$.
Rotor failure can be divided into the structural failure of the rotor and the magnets. Since both are structural failures the same failure rate as mentioned above is assumed. For the bearing failure the distribution of [13] or [14] is examined. The resulting failure rates for the bearing are in the magnitude of $10^{-6} \frac{1}{fh}$ or $10^{-9} \frac{1}{fh}$. As the bearing is a safety critical component for the motor and a jamming could prevent the function of the TRD the lower failure rate is assumed as achievable. For the calculation the results of [1] need to be considered, indicating that at least two functioning winding systems are required to guarantee operation after the loss of one winding system.

Fig 9 illustrates the RBD for the motor itself, the corresponding equation is defined in eq.(3). The calculated failure rate for this system is $1.01 \cdot 10^{-9} \frac{1}{fh}$, highlighting that the failure of the bearing contributes the most to the overall failure rate of the motor.

$$\lambda_{Mot}(t) = \lambda_{Stator}(t) + \lambda_{Winding}(t)^2 + \lambda_{Rotor}(t) + \lambda_{Magnet}(t) + \lambda_{Bearing}(t) \tag{3}$$

After recalculating the failure rate for the triplex motor system, $2.49 \cdot 10^{-9} \frac{1}{fh}$ results as the failure rate for the TRD system and for the benchmark system failure rates of $1.04 \cdot 10^{-8} \frac{1}{fh}$ or $6.68 \cdot 10^{-9} \frac{1}{fh}$ are achieved depending on the ACU placement in the pitch control system.

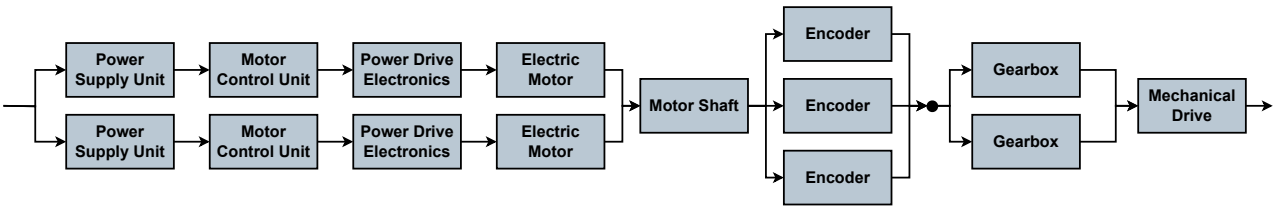

FIG 8. RBD of the tail rotor drive system

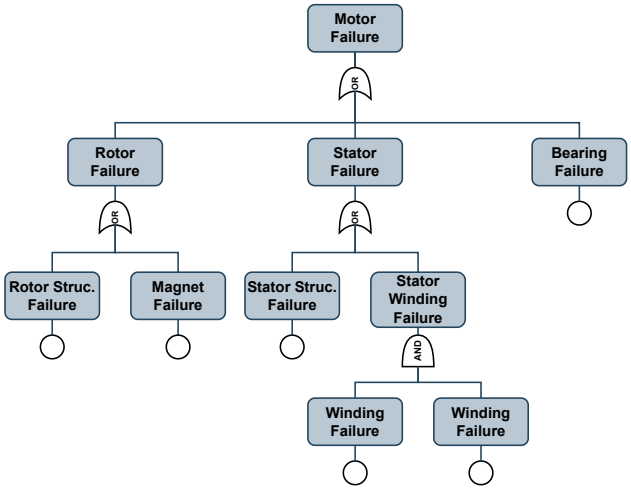

FIG 9. FTA of the triplex motor system

3.2.2. Vertical Stabilizer and Rotor Cover

For the variable stabilizer power electronics, an actuator, a coupling and a rudder are needed. The criticality is estimated with MAJ as it is only used in the en-route segment of the flight mission. Based on the findings of the benchmark system, it can be assumed that a single lane of power electronics is not sufficient and a duplex architecture is necessary. For the actuator, half of the dual duplex actuator can be implemented. The other components don't need redundancy for the system to be sufficiently failure resistant.

For the cover of the rotor the criticality depends on the flight phase. The manoeuvring phase must only be initiated with the cover open, because the closed cover can lead to a CAT event, but if the cover is closed and can't be opened before the manoeuvring phase, an autorotation manoeuvre can be initiated, which is categorised as MAJ. The components required for the closable cover are power electronics, an actuator, a mechanism to link the actuator and cover, and the cover itself. With the insights of chapter 3.2 the same architecture as for the pitch adjustment is choosen. Redundancy is not as easy to implement for the mechanical components as it is for the electrical components. The link mechanism consists of a flexball cable, where the redundancy could be applied in the same way as described for the pitch adjustment or even through a manual cable operated by the pilot. In the event of a failure in the link mechanism that transfers the force, the load paths would have to be decoupled and another one set in place. This would add complexity and weight. Because the required failure rate of the system can't be achieved, a detailed inspection, where different failure modes are investigated, is necessary.

3.2.3. Failure Mode Effects and Criticality Analysis

The Failure Mode Effects and Criticality Analysis (FMECA) is performed for all systems, the TRD, the pitch control, the vertical stabilizer and the closable cover. For each component within these systems, the failure modes are considered, their impacts on the aircraft are described, and methods to migate these effects are identified.

Regarding the TRD system, the analysis indicates the utilization of a single gearbox with appropriate check intervals. No further changes are applied to the system architecture of the benchmark system. This decision is based on the system already being designed to achieve an appropriate failure rate for CAT events.

For the system of the vertical stabilizer and the cover, relevant events are defined along with the faults which are leading to them. For the vertical stabilizer with the adjustable rudder, this is an incorrect rudder deflection.

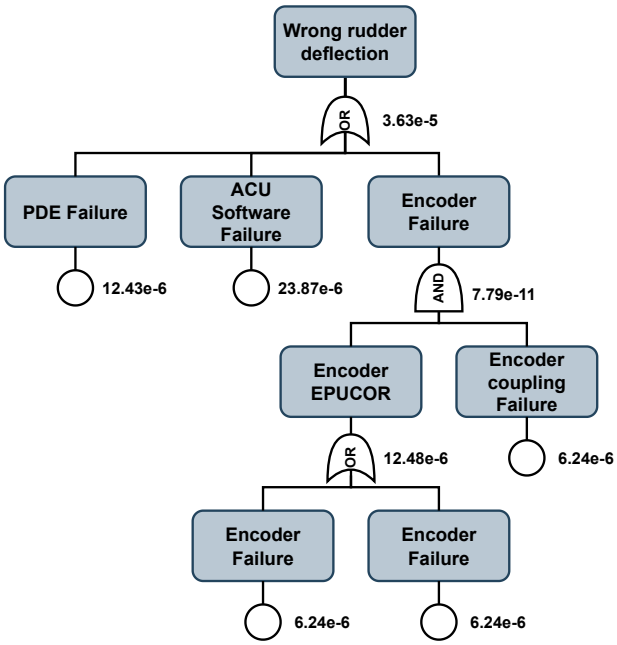

FIG 10. FTA of wrong rudder deflection

As depicted in Fig 10 a failure rate of $3.63 \cdot 10^{-5} \frac{1}{fh}$ is calculated, which exceeds the requirement for MAJ events. However, it is important to note that the failure rate data is sourced from the NPRD, introducing a level

of uncertainty. As long as the failure rate is in the same magnitude, it is considered acceptable.
Another event to consider is a permanently incorrect deflection of the rudder. This event has a failure rate of $7.4 \cdot 10^{-5} \frac{1}{fh}$, with the increase being due to the bearings in the rudder and the clutch. This failure can be compensated for by adjusting the RPM of the electric power train or adjusting the pitch of the rotor blades, and is therefore not critical. If concerns still exist, an oversizing of the components can be performed.

For the closable cover, two relevant events have been identified.
- The cover is not opening. (MAJ)
- The cover is unintentionally closing. (CAT)

There are two internal events for triggering the top event of the cover not opening: the failure of the EMA and the jamming of the cover or link mechanism. It becomes evident that the jamming of the cover predominantly contributed to the occurrence of the top event. Similar to the evaluation of the rudder deflection, the same reasoning is applied here to evaluate the failure rate, resulting in $1.14 \cdot 10^{-5} \frac{1}{fh}$.

The final failure rate for the unintentional closing of the cover accumulates to $1.56 \cdot 10^{-13} \frac{1}{fh}$, which falls below the requirement for CAT events. This is due to the use of a dissimilar redundancy. Two different systems are in place, and both must fail to trigger the top event. The first is the EMA which can hold the cover open. The second is a blocking unit that locks the fully opened cover in place. The combination of these mechanisms significantly mitigates the occurrence of the top event of unintentional cover closing.
Based on the analysis above, it can be deducted that the mechanical components have a considerable impact on the failure rate, and achieving redundancy is more challenging compared to the electric components. The safety considerations for the critical mechanical components, e.g. bearings, must be taken into account at the design phase.

4. SYSTEM MONITORING CONCEPTS

In this section, the monitoring concept is discussed, using the FMECA as its input. Through the identification of relevant fault cases, the components associated with these cases and the physical signals that need to be monitored online can be determined. The following physical signals are considered for monitoring:
- temperature of the motors,
- current and voltage of the motors,
- vibration frequency of the motors, gearboxes and structures,
- torque of the motors and the rotor, and
- position/speed of the components in the controlled system.

One concept of fault detection is the hardware redundancy based one. If a fault in one of the redundantly used components occurs and changes its output, it can be compared and directly isolated [15]. Another option is signal processing. For example the signal processing of the current in the frequency domain can be used to detect electrical, mechanical and demagnetization faults in motors [16]. One disadvantage is that they are mostly used in a steady state and are thus not suitable for online fault detection in dynamic operations. Another option is the analytical redundancy which can describe the behavior in a steady state, as well as in a dynamic process. This can be achieved by using data-driven or physical model based methods. For applying data-driven methods the respective data is not available yet. Physical model based methods can vastly differ in their fidelity, use case and possible online usage.
In [17], the HUMS for a helicopter system is described, including the processing of vibration data, sensor selection, and alarm setup. The monitoring of the vibration signature proves to be an exceptionally potent method, but is currently not applicable for the electric power train system due to the newly installed structures on the tail rotor, which alter the vibration signal from the tail boom. Therefore new tests and data acquisition must be carried out before a vibration signature analysis can be performed.
In the following only monitoring systems for online detection are established, which were defined with the help of the FMECA. These can help mitigate the effects of certain failure modes of components.

4.1. Limit Monitors

For the remaining physical signals, limit monitors can be applied for online monitoring. For the mass short-circuit detection, the potential at the neutral point of each of the 3-phase systems is monitored. The limit value is defined by eq.(4) and results from the accuracy of a current sensor up to 100 amps, which is approximately $\pm 1\%$. i_a,i_b,i_c are the currents of the three phases and $i_{q,max}$ the q-current in the dq0 system, which is the rotating reference frame.

$$i_a + i_b + i_c \geq 0.03 \cdot i_{q,max} \tag{4}$$

Regarding RPM generation, the threshold is defined based on the maximum motor RPM with a buffer of 5% specified in equation (5). The relationship between the actual and monitored motor speed can be considered to be almost one-to-one, since the position encoders used have an accuracy of $\pm 0.15\%$. ω_{EM} is the electric motor speed, ω_{mon} the threshold of the speed and $\omega_{n,max}$ the maximum speed of the motor.

$$\omega_{EM} \geq \omega_{mon} = 0.95 \cdot \omega_{n,max} \tag{5}$$

The position determination of the actuators must be very precise to prevent any mechanical damage to them and can be used as a substitute for speed monitoring. Hence, the threshold is set in close proximity to unity, see eq.(6). φ_{act} is the angle of the EMA, φ_{mon} the respective threshold and φ_{max} the maximum allowable angle of the EMA. The utilization of the same position encoders enables the

achievement of the very low tolerance in the system.

$$\varphi_{act} \geq \varphi_{mon} = 1.01 \cdot \varphi_{max} \tag{6}$$

For the TRD system, a torque monitor for the rotor and motor is also useful to detect component degradation. To calculate the torque at the rotor, the efficiency of the gearbox is required, see eq.(7), with T_{TR} the torque at the tail rotor, T_{motor} the torque of the motor, $\eta_{gearbox}$ as the gearbox efficiency and GR as the gearbox ratio. The accuracy of torque sensors can range from $\pm 0.15\%$ to $\pm 2\%$.

$$T_{TR} = \eta_{gearbox} \cdot T_{motor} \cdot GR \tag{7}$$

An initial estimation for the efficiency of the gearbox can be made using a regression formula from [18], see eq(8). PR represents the applied power rating of the gearbox. With this estimation and the accuracy of the torque sensors, a torque monitoring system can be implemented.

$$\eta_{gearbox} = 0.989 \cdot PR^{0.0135} \tag{8}$$

In terms of fault detection for the degradation of the actuator in the rudder, cover, and pitch control systems, the required current in the motors can be monitored in conjunction with position monitoring. This combination can be used to detect degradation, incorrect output, or faults such as jamming, as described in equation (9), with $i_{a,b,c}$ as the current of the phases of the motors in the EMA.

$$i_{a,b,c} \geq i_{mon} = 1.1 \cdot i_{q,max} \tag{9}$$

Furthermore a limit value for the temperature in the motors has to be defined. This depends on the material used for the permanent magnets and the winding. The temperature is set to $150°C$. If the threshold temperature is exceeded demagnetization will occur leading to loss of torque generation.

4.2. Analytical redundancy

With the analytical redundancy additional monitors can be used to perform online fault detection and isolation. This method relies on defining the necessary dependencies of physical signals. Tab. 4 presents the dependencies between the electrical and mechanical domains. Constants such as back EMF constant k_E and torque constant k_T can be measured for motors and used to calculate torque T_m or speed ω_m from electrical values [19], see eq.(10) with U_{motor} as the induced voltage and eq.(11) with I_{motor} as the rms current. To fully utilize these equations, the efficiency of the motor must also be known. The efficiency can be determined through FEM calculations, tests, or using the method described in [20], which is validated for a machine in a similar power region to that used in the tail rotor. The efficiency of the motor depends on the torque and speed of the motor as shown in equation (12), with ΔP as the resulting losses at the operating point. With these simple monitors online detection can be easily realized and a degradation can be detected.

Domain	Physical Signal	
Mechanical	Torque	Velocity
Electrical	Current	Voltage

TAB 4. Dependencies of physical signals

The torque at the tail rotor T_{TR} can be estimated using equation (13).

$$\omega_m = U_{motor,induced} \cdot k_E \tag{10}$$

$$T_m = I_{motor} \cdot k_T \tag{11}$$

$$\eta_{motor} = \frac{T_m \cdot \omega_m}{T_m \cdot \omega_m + \Delta P(T, \omega_m)} \tag{12}$$

$$T_{TR} = T_m \cdot \eta_{gearbox} \cdot \eta_{motor} \cdot GR \tag{13}$$

The described analytical redundancy can be applied for the TRD system but also to the pitch control system, rudder and closable cover systems.

5. SUMMARY AND CONCLUSION

In this paper, the design of an electric power train for a tail rotor was reviewed from a safety aspects, as well as a condition monitoring perspective. Although it is possible to certify the system individually, it is advisable to closely collaborate with the aircraft manufacturer, as the safety requirements for the EHPS directly correlate with the AFHA.

Redundancy, particularly in the electric systems, plays a crucial role in meeting the safety requirements for failure rates. Special attention is given to the electric motor in the TRD system, as it is a triple redundant motor housed in a single unit, which requires special considerations. In the event of a short circuit in the motor system, a breaking torque may occur. Since a duplex system cannot overcome this breaking torque, a triplex system is necessary.

For the vertical stabilizer with an adjustable rudder and the closable cover a FEMCA and FTA are utilized to define the critical events and determine their respective failure rates. Via the safety assessment, it becomes evident that mechanical components contribute significantly to the overall system failure rate and that a safe-life design of these components may be necessary.

A system monitoring concept is described, emphasizing the potential for online fault detection. Fault detection can be accomplished by monitoring the electric power required by the systems. If the power consumption exceeds a predefined threshold, system degradation can be assumed. Additionally, a sensor network enables fault

isolation. Analytical redundancy is also discussed to aid detecting failures and degradation in the motor or gearbox. More detailed models are being developed for fault detection and isolation. The proposed monitoring concepts with the models will be validated in the future with simulations in MATLAB® Simulink and compared with a demonstrator for the tail rotor. With this the thresholds and necessary residuals will be reviewed and if necessary adjusted.
In conclusion, an electric power train for an electric tail rotor is feasible. These considerations can also be transferred on other applications, e.g. the propulsion system for a electrical aircraft.

ACKNOLEDGMENT

The results of the presented paper are part of the work in the research project "Hubschrauber-Heckausleger mit elektrisch angetriebener Schuberzeugung und -steuerung" (eTail), which is supported by the Federal Ministry of Economic Affairs and Climate Action in the national LuFo VI-1 program. Any opinions, findings and conclusions expressed in this document are those of the authors and do not necessarily reflect the views of the other project partners.

Supported by:

Federal Ministry
for Economic Affairs
and Climate Action

on the basis of a decision
by the German Bundestag

Contact address:

stefan.hibler@tuhh.de

References

[1] Martin Stoll, Uwe T.P. Arnold, Christopher Hupfer, Christoph Stuckmann, Stephan Bichlmaier, Maximilian Mindt, Susanne Seher-Weiß, Stefan Hibler, and Frank Thielecke. Full electric helicopter anti-torque. In *48th European Rotorcraft Forum*, September 2022.

[2] S-18 Aircraft; Sys Dev; Safety Assessment Committee. Guidelines and methods for conducting the safety assessment process on civil airborne systems and equipment. Technical report, 1996.

[3] European Union Aviation Safety Agency (EASA). CRI Consultation paper Special Condition. SC E-19. Technical report, February 2023.

[4] European Union Aviation Safety Agency (EASA). Certification Specifications, Acceptable Means of Compliance and Guidance Material for Small Rotorcraft. CS-27. Amendment 9. Technical report, 2021.

[5] European Union Aviation Safety Agency (EASA). Information session on EASA Electrical Hybrid Propulsion System (EHPS). Technical report, June 2021.

[6] S-18 Aircraft; Sys Dev; Safety Assessment Committee. Guidelines for Development of Civil Aircraft and Systems. Technical report, 2010.

[7] RTCA, Inc. RTCA/DO-160F - Environmental Conditions and Test Procedures for Airborne Equipment. Technical report, 2007.

[8] RTCA, Inc. RTCA DO-254 / EUROCAE ED-80, Design Assurance Guidance for Airborne Electronic Hardware. Technical report, 2000.

[9] RTCA, Inc. RTCA/DO-178C, Software Considerations in Airborne Systems and Equipment Certification. Technical report, 2012.

[10] John Reade David Mahar, William Fields. Nonelectronic Parts Reliability Data - NPRD-2016. Technical report, QUANTERION SOLUTIONS INCORPORATED, 2015.

[11] M. Desai, J. Deckert, J. Deyst, A. Willsky, and E. Chow. Dual redundant sensor fdi techniques applied to the nasa f8c dfbw aircraft. In *Guidance and Control Conference*, Reston, Virigina, 1976. American Institute of Aeronautics and Astronautics. DOI: 10.2514/6.1976-1976.

[12] Department of Defense. MIL-HDBK-217F, Military Handbook: Reliabilty Prediction of Electronic Equipment. Technical report, 1991.

[13] Department of Defense. MIL-HDBK-338B, Military Handbook: Electronic Reliabilty Design. Technical report, 1998.

[14] Gianpietro Di Rito, Roberto Galatolo, and Francesco Schettini. Self-monitoring electro-mechanical actuator for medium altitude long endurance unmanned aerial vehicle flight controls. *Advances in Mechanical Engineering*, 8(5):1687814016644576, 2016. DOI: 10.1177/1687814016644576.

[15] Steven X. Ding. *Model-Based Fault Diagnosis Techniques*. Springer London, London, 2013. ISBN: 978-1-4471-4798-5. DOI: 10.1007/978-1-4471-4799-2.

[16] Zhifu Wang, Jingzhe Yang, Huiping Ye, and Wei Zhou. A review of permanent magnet synchronous motor fault diagnosis. In *2014 IEEE Conference and Expo Transportation Electrification Asia-Pacific (ITEC Asia-Pacific)*, pages 1–5, 2014. DOI: 10.1109/ITEC-AP.2014.6940870.

[17] Kenneth Pipe. *Health and Usage Monitoring Systems (HUM Systems) for Helicopters: Architecture and Performance*. 2009. ISBN: 9780470061626. DOI: 10.1002/9780470061626. shm127.

[18] Stefan Stückl. *Methods for the Design and Evaluation of Future Aircraft Concepts Utilizing Electric Propulsion Systems*. PhD thesis, Technische Universität München, 2016.

[19] J.R. Hendershot and T.J.E. Miller. *Design of Brushless Permanent-magnet Motors*. Magna physics publications. Magna Pysics Pub., 1994. ISBN: 9780198593898.

[20] Martin Novak, Jaroslav Novak, Zdenek Novak, Jan Chysky, and Oleg Sivkov. Efficiency mapping of a 100 kw pmsm for traction applications. In *2017 IEEE 26th International Symposium on Industrial Electronics (ISIE)*, pages 290–295, 2017. DOI: 10.1109/ISIE.2017.8001262.